Electronic Supplementary Information

All-inkjet-printed, solid-state flexible supercapacitors on paper

Keun-Ho Choi,[a] JongTae Yoo,[ab] Chang Kee Lee[c] and Sang-Young Lee[a]*

[a]*Department of Energy Engineering, School of Energy and Chemical Engineering, Ulsan National Institute of Science and Technology (UNIST), Ulsan, 689-798, South Korea. E-mail: syleek@unist.ac.kr; Tel: +82-52-217-2948*

[b]*School of Energy and Chemical Engineering, Ulsan National Institute of Science and Technology (UNIST), Ulsan, 689-798, South Korea.*

[c]*Korea Packaging Center, Korea Institute of Industrial Technology, Bucheon, Gyeonggi-do, 421-742, South Korea.*

Fig. S1. Schematics and SEM images of the stepwise fabrication procedure of the CNF nanomat-based primer layer: (a) A4 paper, (b) inkjet-printed (wet-state) CNF layer deposited on A4 paper, (c) inkjet-printed CNF nanomat deposited onto A4 paper. The highly developed nanoporous structure was generated after the solvent exchange between ethanol/acetone mixture and water.

Fig. S2. 3D laser scanning microscope images of: (a) A4 paper (wetting substrate, R_a (surface roughness) ~ 4.8 μm) and (b) PET film (non-wetting substrate, R_a ~ 0.2 μm).

Fig. S3. Viscosity of the electrode (SWNT/AC) inks as a function of shear rate, before/after centrifugation (at 10,000 rpm for 1 h).

Fig. S4. SEM images of the Ag NWs: (a) before and (b) after sonication-driven scission.

Fig. S5. Viscosity of Ag NW inks (containing short NWs, after sonication-driven scission) as a function of shear rate.

Fig. S6. SEM images of a control sample (Ag NWs without SWNTs): (a) before and (b) after UV irradiation.

Fig. S7. FT-IR spectra showing the change of characteristic peaks assigned to C=C double bonds of ETPTA, before/after the UV crosslinking reaction.

Fig. S8. Linear sweep voltammetry (LSV) profile of [BMIM][BF_4]/ETPTA mixture (after removal of the residual water).

Fig. S9. TGA profile (dynamic mode, heating rate = 10 ^oC min^{-1} under nitrogen atmosphere) of the inkjet-printed ([BMIM][BF_4]/ETPTA) solid-state electrolyte.

Fig. S10. Effect of scan rates (= 1 - 200 mV s^{-1}) on: (a) CV profiles and (b) coulombic efficiency of the inkjet-printed SC.

Fig. S11. Ragone plot (*i.e.*, specific energy density [Wh kg^{-1}] vs. specific power density [W kg^{-1}]) of the inkjet-printed SC.

Fig. S12. (a) Galvanostatic charge-discharge (GCD) profiles (at current density = 0.2 mA cm^{-2}) of the inkjet-printed SCs showing IR drop. Galvanostatic GCD profiles (at current densities = 1.0 – 10.0 mA cm^{-2}) of the inkjet-printed SCs (b) with Ag NWs and (c) without Ag NWs.

Fig. S13. Schematics and photographs of the inkjet-printed SCs: (a) 5 cells connected in series and (b) 5 cells connected in parallel.

Fig. S14. (a) Schematic of the inkjet-printed, letter ("BATTERY")-shaped SC that was seamlessly connected with the inkjet-printed electrical circuit. (b) Charge/discharge profiles of the inkjet-printed, letter ("BATTERY")-shaped SC.

Fig. S15. (a) Schematic of the inkjet-printed, traditional Korean "Taegeuk" symbol-like SC that was aesthetically unitized with inkjet-printed electric circuit and other patterns. (b) Charge/discharge profiles of the inkjet-printed, "Taegeuk" symbol-like SC.

Fig. S16. A schematic of the inkjet-printed SCs that were seamlessly connected via the inkjet-printed electric circuits to LED lamps in the inkjet-printed Korea map.

Fig. S17. Photographs of the (a) temperature sensor and (b) Arduino board.

Fig. S18. Video clips showing the operation of: (a) a blue LED lamp in the smart cup (for cold water (~ 10 ^{o}C)) and (b) a red LED lamp in the smart cup (for hot water (~ 80 ^{o}C)).

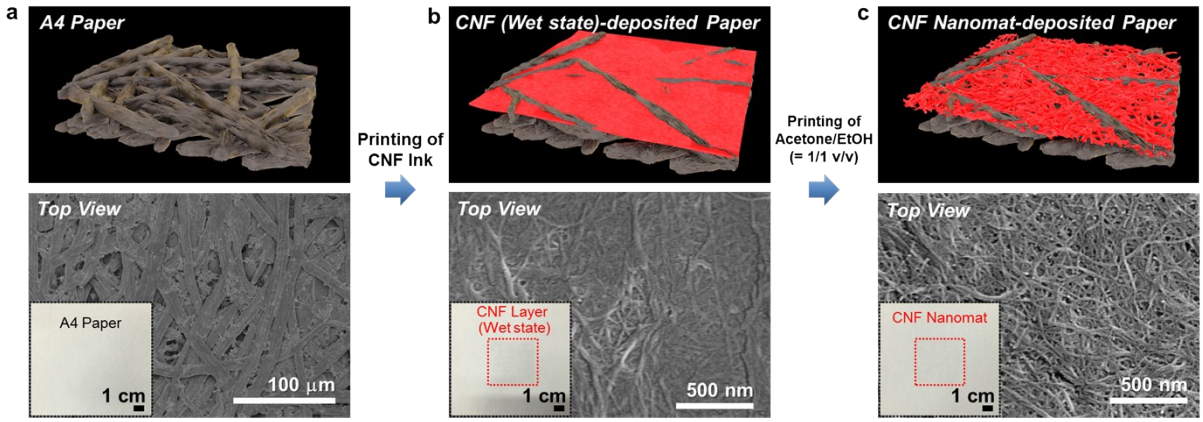

Fig. S1. Schematics and SEM images of the stepwise fabrication procedure of the CNF nanomat-based primer layer: (a) A4 paper, (b) inkjet-printed (wet-state) CNF layer deposited on A4 paper, (c) inkjet-printed CNF nanomat deposited onto A4 paper. The highly developed nanoporous structure was generated after the solvent exchange between ethanol/acetone mixture and water.

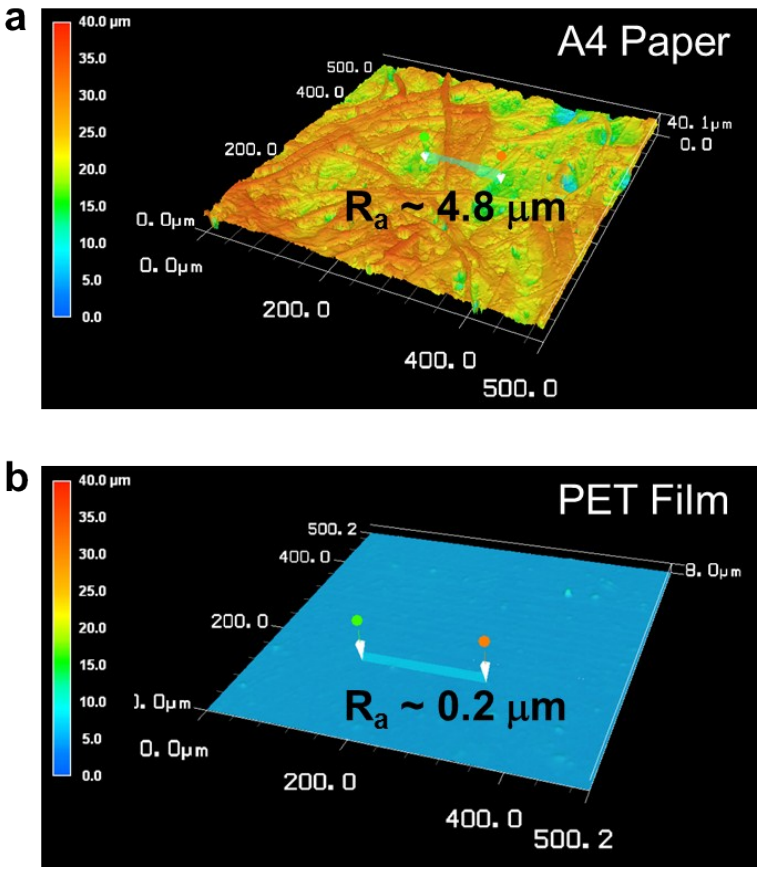

Fig. S2. 3D laser scanning microscope images of: (a) A4 paper (wetting substrate, R_a (surface roughness) ~ 4.8 µm) and (b) PET film (non-wetting substrate, R_a ~ 0.2 µm).

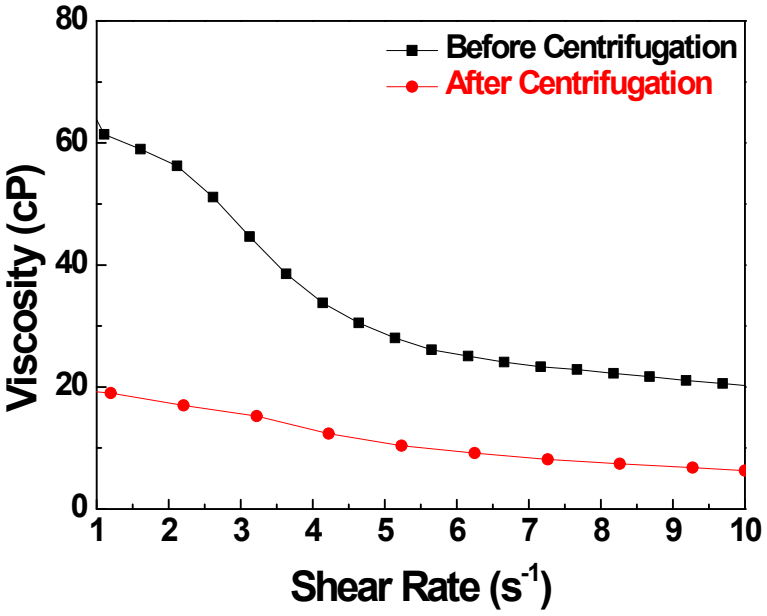

Fig. S3. Viscosity of the electrode (SWNT/AC) inks as a function of shear rate, before/after centrifugation (at 10,000 rpm for 1 h).

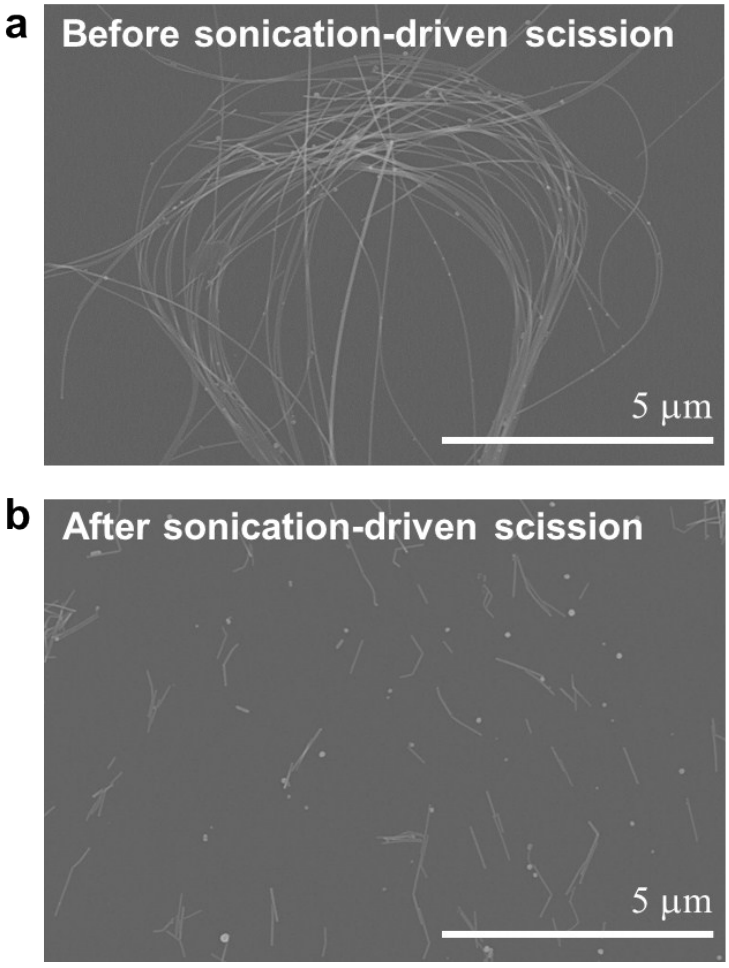

Fig. S4. SEM images of the Ag NWs: (a) before and (b) after sonication-driven scission.

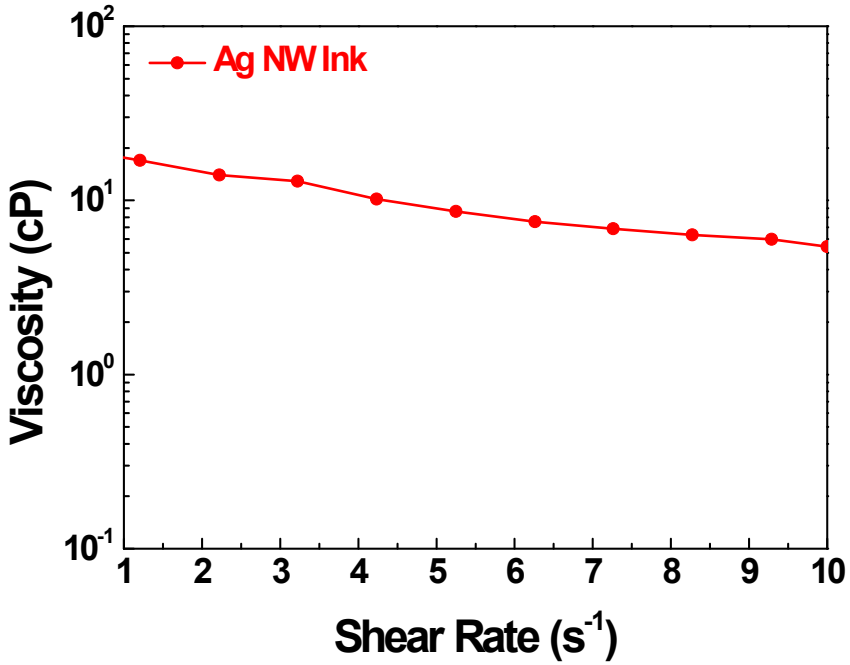

Fig. S5. Viscosity of Ag NW inks (containing short NWs, after sonication-driven scission) as a function of shear rate.

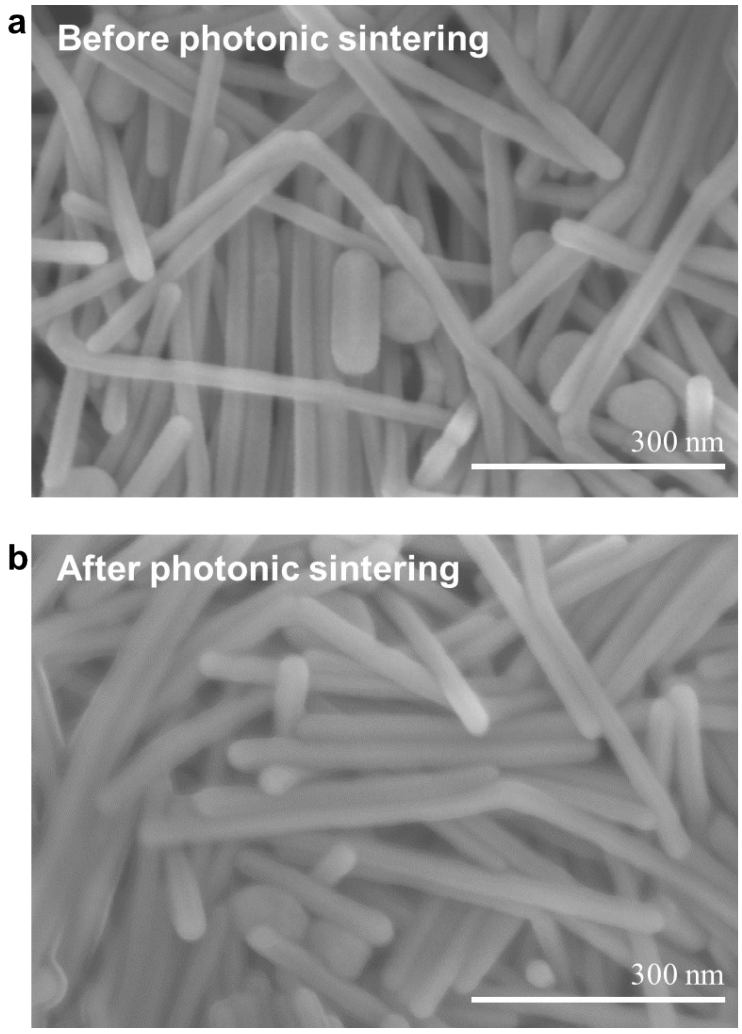

Fig. S6. SEM images of a control sample (Ag NWs without SWNTs): (a) before and (b) after UV irradiation.

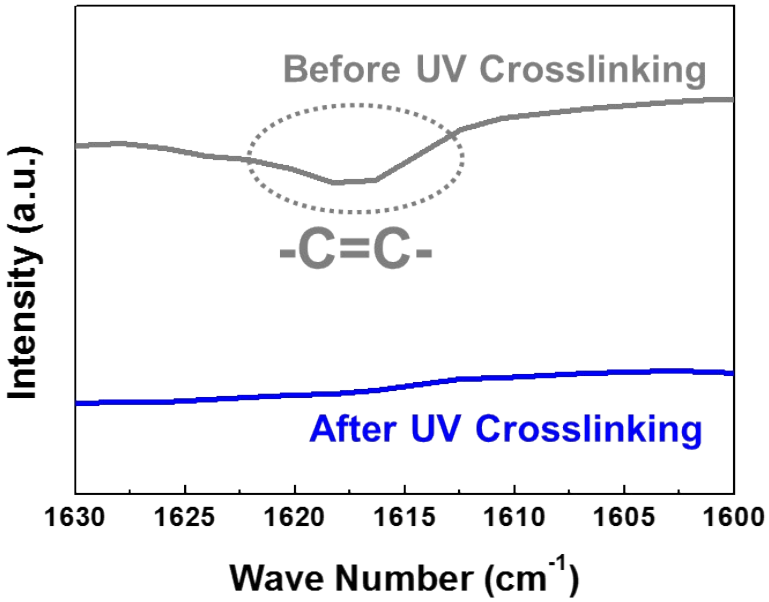

Fig. S7. FT-IR spectra showing the change of characteristic peaks assigned to C=C double bonds of ETPTA, before/after UV crosslinking reaction.

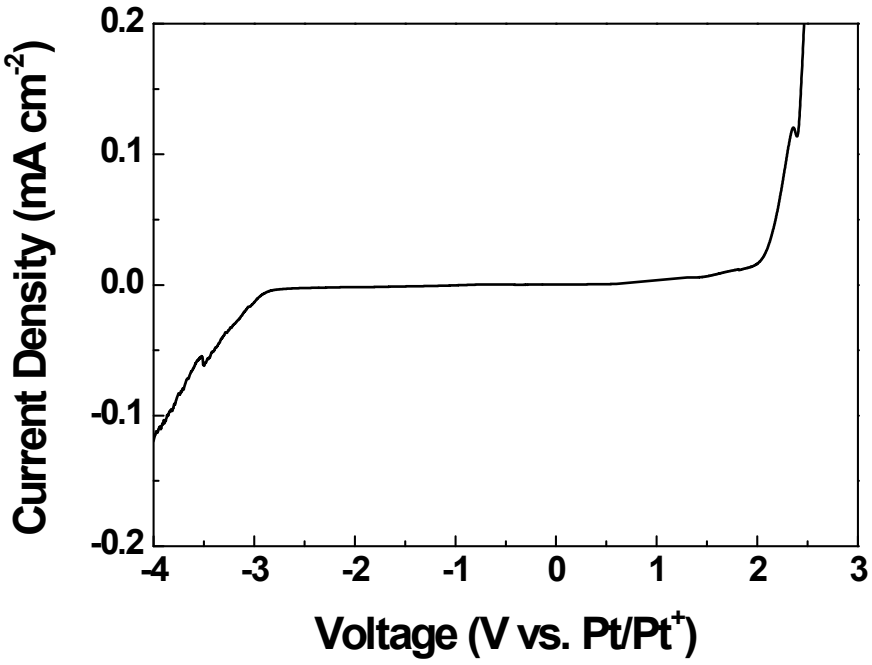

Fig. S8. Linear sweep voltammetry (LSV) profile of [BMIM][BF_4]/ETPTA mixture (after removal of the residual water).

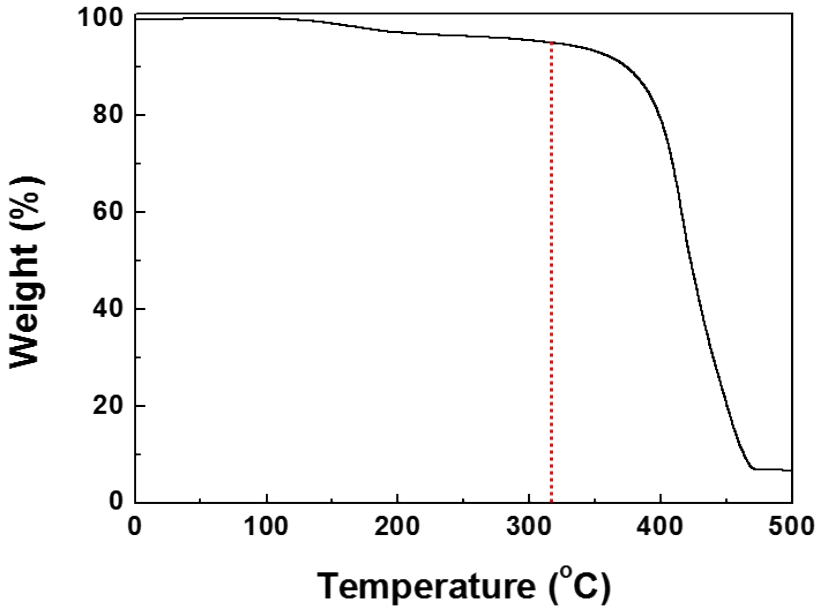

Fig. S9. TGA profile (dynamic mode, heating rate = 10 ^{o}C min^{-1} under nitrogen atmosphere) of the inkjet-printed ([BMIM][BF_4]/ETPTA) solid-state electrolyte.

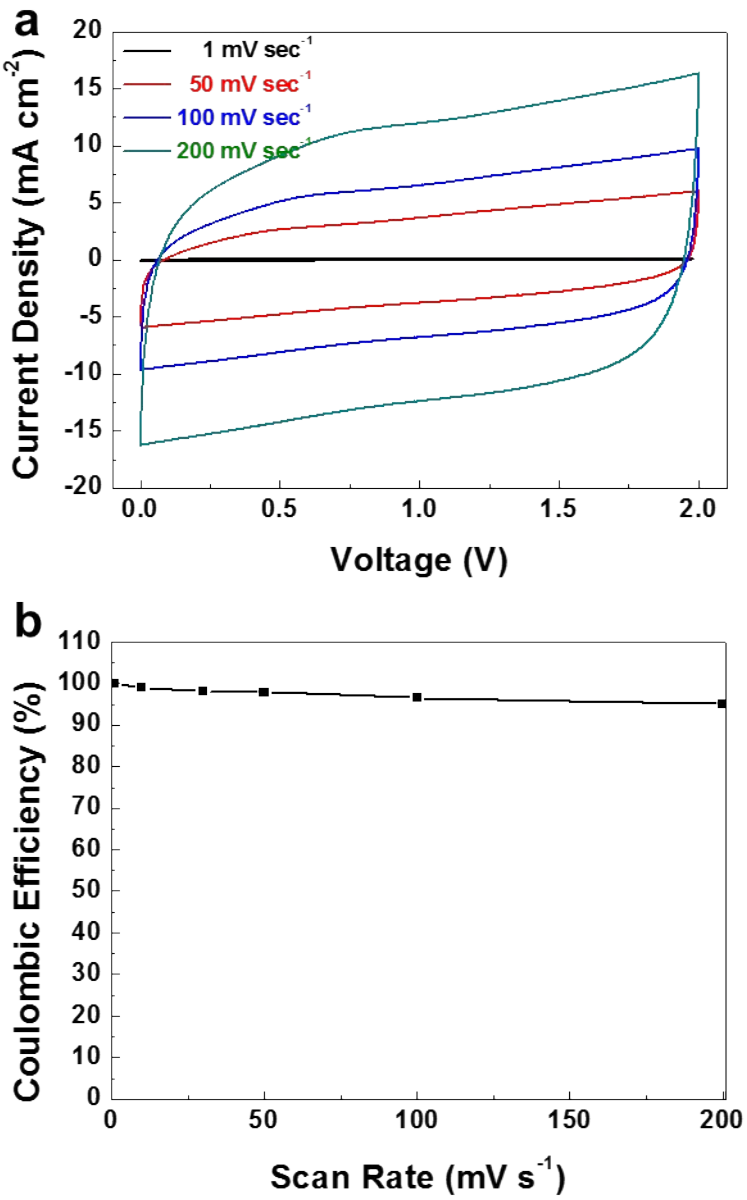

Fig. S10. Effect of scan rates (= 1 - 200 mV s^{-1}) on: (a) CV profiles and (b) coulombic efficiency of the inkjet-printed SC.

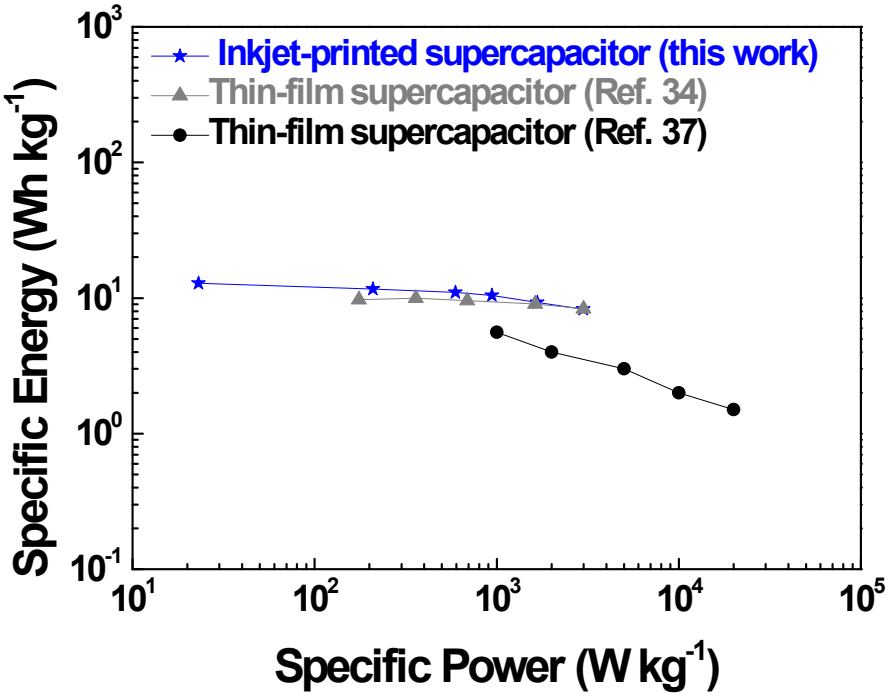

Fig. S11. Ragone plot (*i.e.*, specific energy density [Wh kg^{-1}] vs. specific power density [W kg^{-1}]) of the inkjet-printed SC.

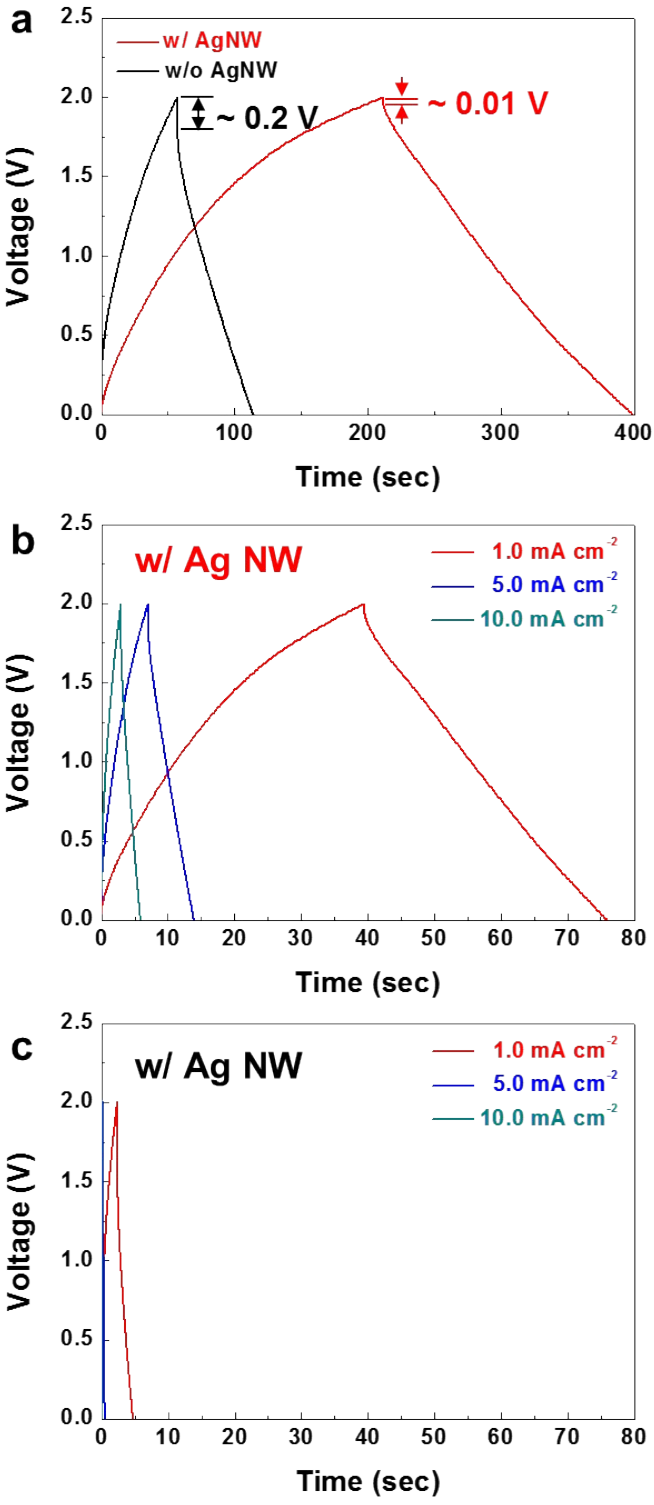

Fig. S12. (a) Galvanostatic charge-discharge (GCD) profiles (at current density = 0.2 mA cm^{-2}) of the inkjet-printed SCs showing IR drop. Galvanostatic GCD profiles (at current densities = 1.0 – 10.0 mA cm^{-2}) of the inkjet-printed SCs (b) with Ag NWs and (c) without Ag NWs.

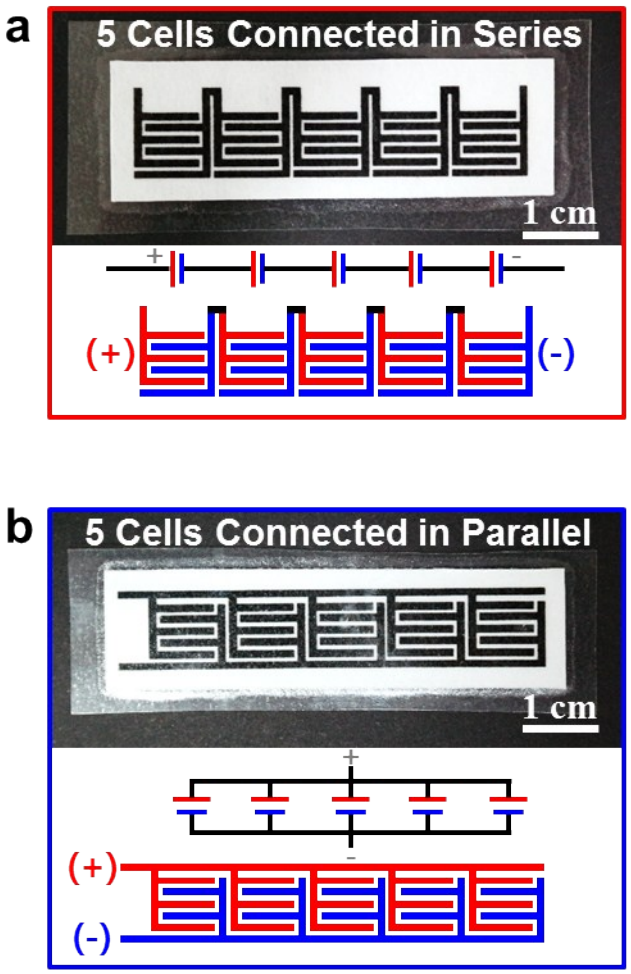

Fig. S13. Schematics and photographs of the inkjet-printed SCs: (a) 5 cells connected in series and (b) 5 cells connected in parallel.

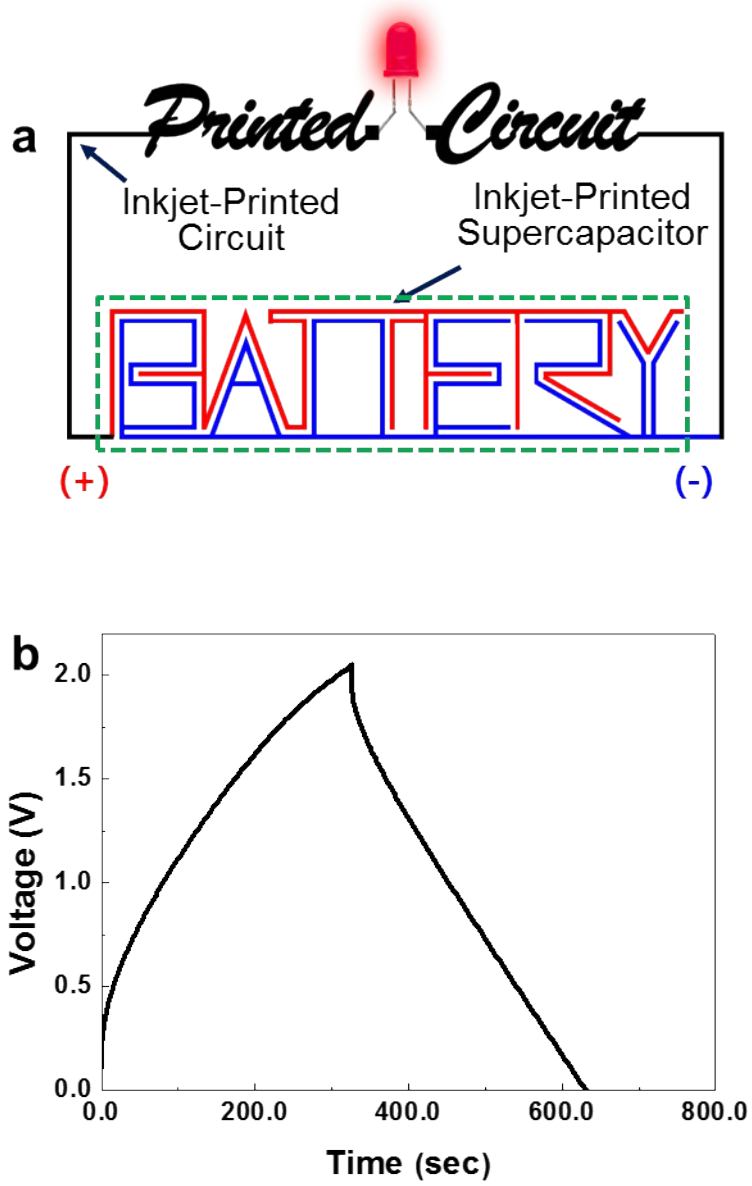

Fig. S14. (a) Schematic of the inkjet-printed, letter ("BATTERY")-shaped SC that was seamlessly connected with the inkjet-printed electrical circuit. (b) Charge/discharge profiles of the inkjet-printed, letter ("BATTERY")-shaped SC.

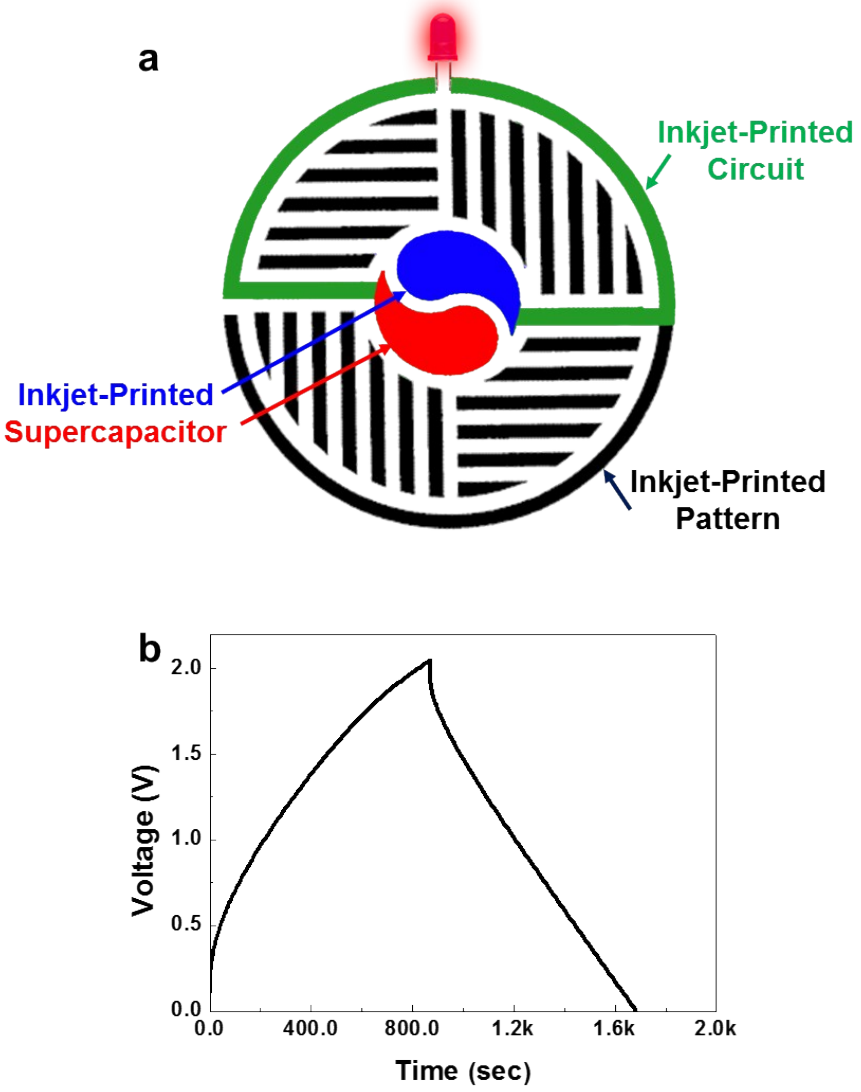

Fig. S15. (a) Schematic of the inkjet-printed, traditional Korean "Taegeuk" symbol-like SC that was aesthetically unitized with the inkjet-printed electric circuit and other patterns. (b) Charge/discharge profiles of the inkjet-printed, "Taegeuk" symbol-like SC.

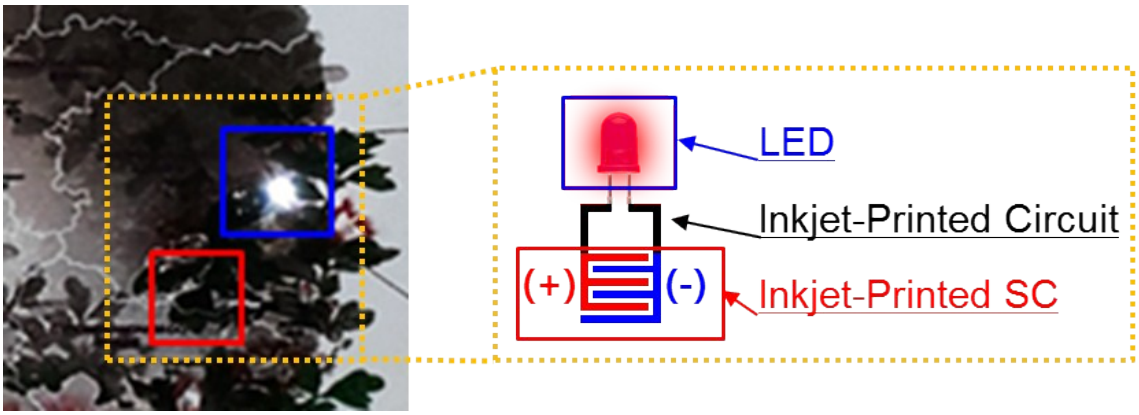

Fig. S16. Schematic of the inkjet-printed SCs that were seamlessly connected via the inkjet-printed electric circuits to LED lamps in the inkjet-printed Korea map.

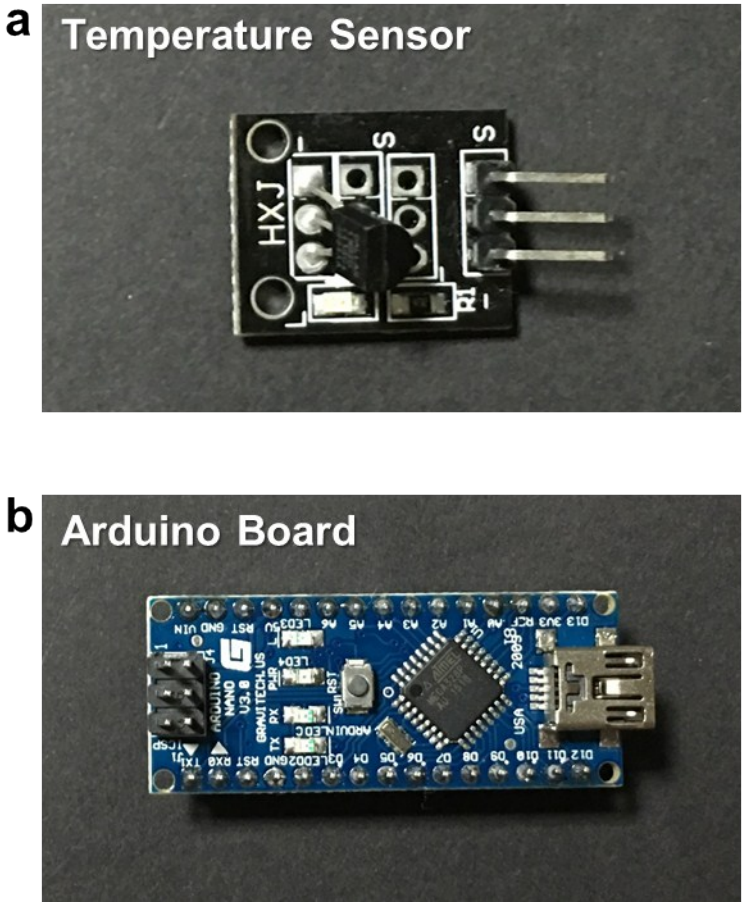

Fig. S17. Photographs of the (a) temperature sensor and (b) Arduino board.

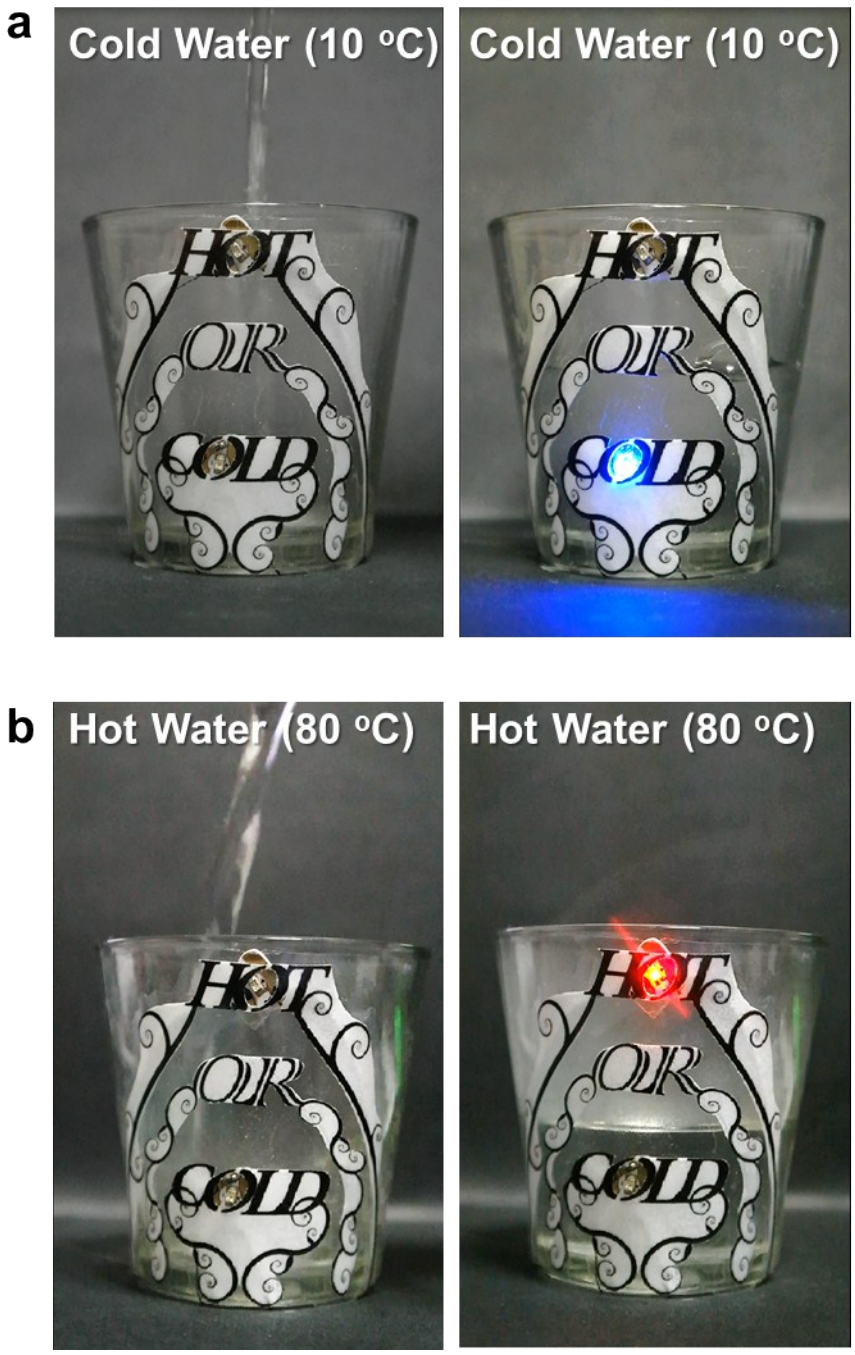

Fig. S18. Video clips showing the operation of: (a) a blue LED lamp in the smart cup (for cold water (~ 10 °C)) and (b) a red LED lamp in the smart cup (for hot water (~ 80 °C)).